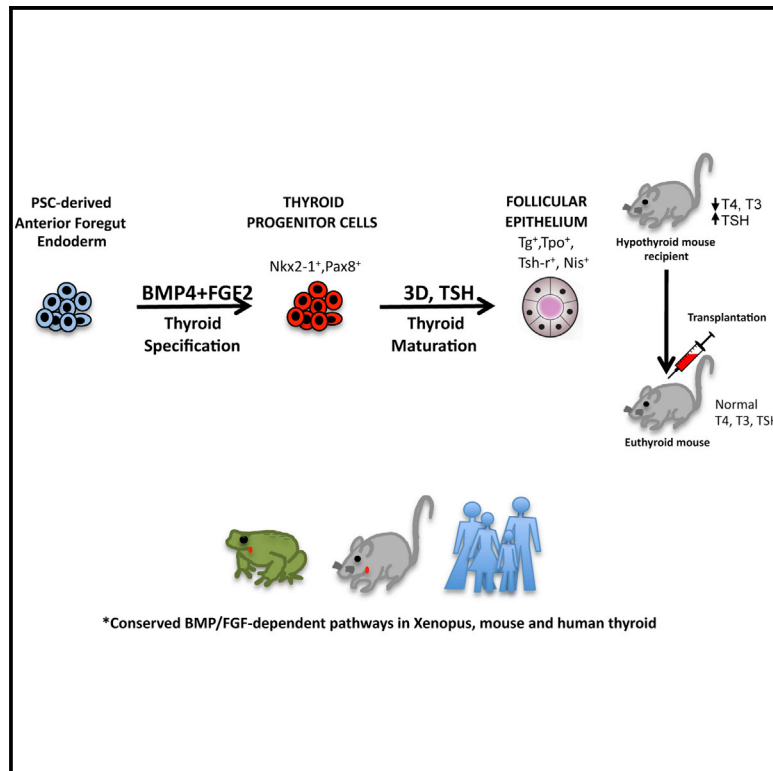


Regeneration of Thyroid Function by Transplantation of Differentiated Pluripotent Stem Cells

Graphical Abstract



Authors

Anita A. Kurmann, Maria Serra, Finn Hawkins, ..., Aaron M. Zorn, Anthony N. Hollenberg, Darrell N. Kotton

Correspondence

thollenb@bidmc.harvard.edu (A.N.H.), dkotton@bu.edu (D.N.K.)

In Brief

The molecular pathways governing thyroid differentiation are poorly understood. Kurmann et al. show that BMP4 and FGF2 activate key pathways that drive thyroid specification *in vivo* and *in vitro*, enabling differentiation of mouse and human pluripotent stem cells into thyroid follicular cells that produce thyroid hormones and rescue mouse hypothyroidism.

Highlights

- BMP4 and FGF2 are necessary and sufficient to specify the thyroid lineage
- Pathways regulating thyroid specification are conserved across species
- Transplantation of ESC-derived thyroid cells regenerates *in vivo* function
- Patient-specific thyroid progenitors can be differentiated from human iPSCs

Regeneration of Thyroid Function by Transplantation of Differentiated Pluripotent Stem Cells

Anita A. Kurmann,^{1,2,10} Maria Serra,^{2,3,10} Finn Hawkins,^{2,3} Scott A. Rankin,⁴ Munemasa Morj,^{2,3} Inna Astapova,¹ Soumya Ullas,⁶ Sui Lin,⁵ Melanie Bilodeau,⁷ Janet Rossant,^{7,8} Jyh C. Jean,^{2,3} Laertis Ikononou,^{2,3} Robin R. Deterding,⁹ John M. Shannon,⁵ Aaron M. Zorn,⁴ Anthony N. Hollenberg,^{1,11,*} and Darrell N. Kotton^{2,3,11,*}

¹Division of Endocrinology, Diabetes and Metabolism, Beth Israel Deaconess Medical Center and Harvard Medical School, Boston, MA 02215, USA

²Center for Regenerative Medicine, Boston University and Boston Medical Center, Boston, MA 02118, USA

³The Pulmonary Center and Department of Medicine, Boston University School of Medicine, Boston, MA 02118, USA

⁴Division of Developmental Biology, Perinatal Institute

⁵Division of Pulmonary Biology

Cincinnati Children's Hospital, Cincinnati, OH 45229, USA

⁶Longwood Small Animal Imaging Facility, Beth Israel Deaconess Medical Center, Boston, MA 02215, USA

⁷Program in Developmental and Stem Cell Biology, Peter Gilgan Centre for Research and Learning, The Hospital for Sick Children, Toronto, ON M5G 0A4, Canada

⁸Department of Molecular Genetics, University of Toronto, Toronto, ON M5S 1A8, Canada

⁹Breathing Institute at the Children's Hospital Colorado and Section of Pediatric Pulmonary Medicine, University of Colorado Denver, Aurora, CO 80045, USA

¹⁰Co-first author

¹¹Co-senior author

*Correspondence: thollenb@bidmc.harvard.edu (A.N.H.), dkotton@bu.edu (D.N.K.)

<http://dx.doi.org/10.1016/j.stem.2015.09.004>

SUMMARY

Differentiation of functional thyroid epithelia from pluripotent stem cells (PSCs) holds the potential for application in regenerative medicine. However, progress toward this goal is hampered by incomplete understanding of the signaling pathways needed for directed differentiation without forced overexpression of exogenous transgenes. Here we use mouse PSCs to identify key conserved roles for BMP and FGF signaling in regulating thyroid lineage specification from foregut endoderm in mouse and *Xenopus*. Thyroid progenitors derived from mouse PSCs can be matured into thyroid follicular organoids that provide functional secretion of thyroid hormones in vivo and rescue hypothyroid mice after transplantation. Moreover, by stimulating the same pathways, we were also able to derive human thyroid progenitors from normal and disease-specific iPSCs generated from patients with hypothyroidism resulting from NKX2-1 haploinsufficiency. Our studies have therefore uncovered the regulatory mechanisms that underlie early thyroid organogenesis and provide a significant step toward cell-based regenerative therapy for hypothyroidism.

INTRODUCTION

Recent progress in the differentiation of pluripotent stem cells (PSCs) in vitro has allowed the derivation of desired cell lineages

and in some instances their in vitro self-assembly into 3D structures, referred to as organoids (Lancaster and Knoblich, 2014; McCracken et al., 2014). Transplantation and in vivo function of engineered cells has been less successful, typically because of poor engraftment. The derivation of PSC-derived endocrine tissues, such as pancreatic islets or thyroid follicles, provides particularly attractive opportunities to achieve in vivo function without orthotopic transplantation, because engraftment of these hormone-secreting tissues in any location with access to circulating blood would potentially achieve function and even clinical rescue of hormone deficiency. Indeed, the differentiation of PSCs into pancreatic islet-like cells has produced cells able to secrete insulin in vivo following transplantation (Pagliuca et al., 2014). In marked contrast, thyroid epithelial cells displaying in vivo functional potential have been generated from PSCs only through forced overexpression of transcription factors (Antonica et al., 2012; Ma et al., 2013, 2015). The directed differentiation of PSCs in vitro into thyroid epithelial cells using growth factor-supplemented media previously has resulted only in immature cells that fail to express the full genetic program necessary for functional thyroid hormone biosynthesis (Arufe et al., 2006, 2009; Jiang et al., 2010; Longmire et al., 2012; Ma et al., 2009).

The primary hurdle preventing the successful differentiation of PSCs into mature thyroid cells has been a lack of knowledge of the pathways that regulate early thyroid embryonic development. "Directed differentiation" of PSCs involves sequential exposure of undifferentiated PSCs to a series of growth factor-supplemented media designed to recapitulate the sequence of developmental milestones that normally occurs during embryonic differentiation. This approach has been used to successfully produce a wide variety of non-thyroid lineages from PSCs (Murry

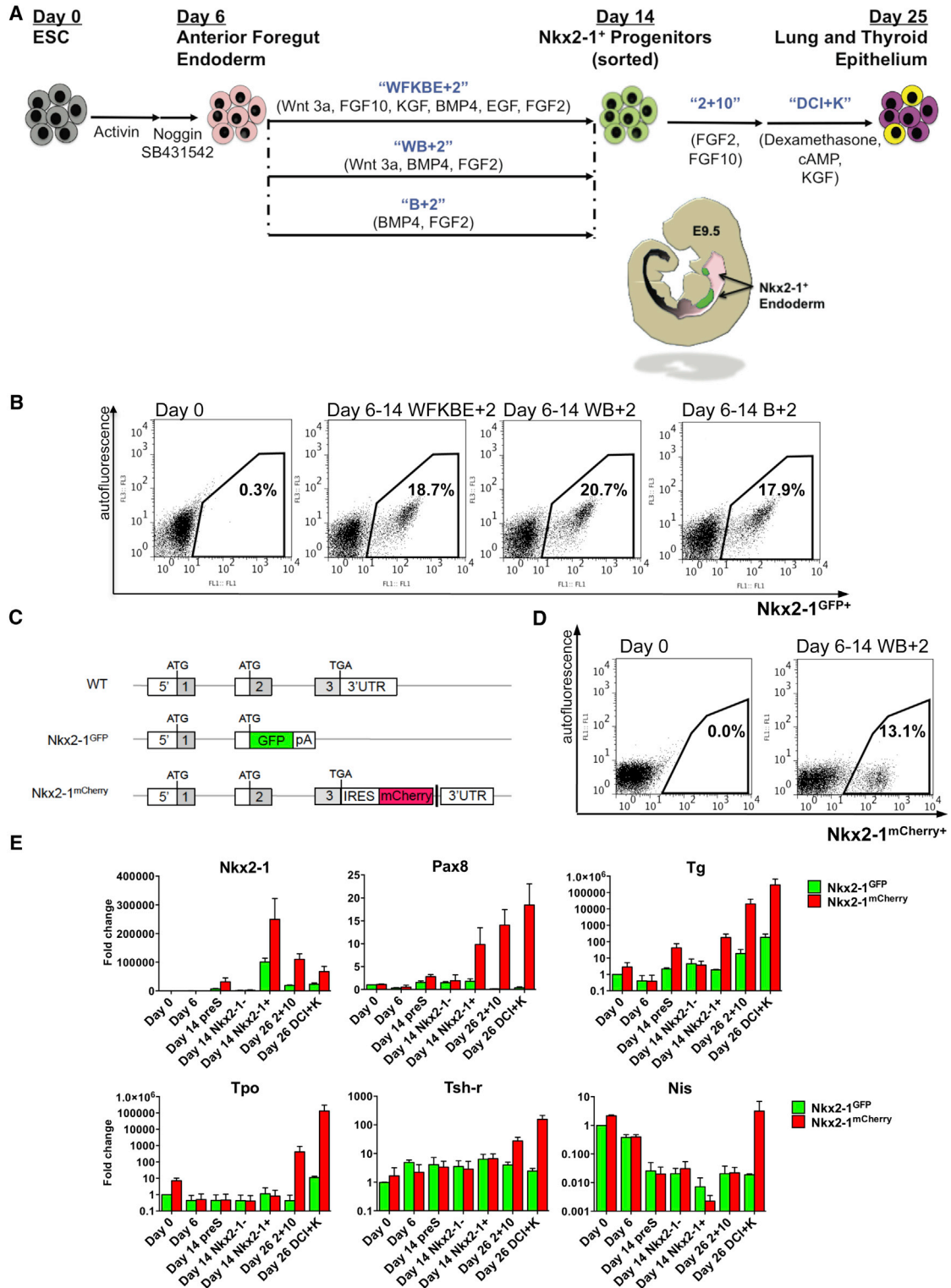


Figure 1. Exogenous BMP4 and FGF2 Are Sufficient to Specify Nkx2-1⁺ Thyroid Progenitors from ESC-Derived Endoderm

(A) Schematic comparing protocols for directed differentiation of mouse ESCs into Nkx2-1⁺ cells.

(B) Representative sort gates used to purify Nkx2-1^{GFP+} cells on day 14, showing efficiency of specification in each media.

(C) Schematic of wild-type (WT) versus targeted Nkx2-1 alleles in the Nkx2-1^{GFP} and Nkx2-1^{mCherry} reporter ESC lines. Boxes represent exons. IRES, internal ribosomal entry site; pA, polyadenylation site.

(legend continued on next page)

and Keller, 2008). The derivation of thyroid epithelial cells via directed differentiation remains a compelling goal given the known capacity of thyroid epithelia to self-organize and form follicular structures in vitro (Hilfer et al., 1968; Mallette and Anthony, 1966). Moreover, recent work has demonstrated that thyroid cells generated from embryonic stem cells (ESCs) through forced overexpression of transcription factors also formed follicles in vitro or after transplantation in vivo (Antonica et al., 2012; Ma et al., 2015).

Here we identify combinatorial bone morphogenetic protein (BMP) and fibroblast growth factor (FGF) signaling as necessary to induce thyroid fate in developing anterior foregut endoderm in multiple species, from amphibians to humans, and we use these pathways to induce thyroid fate in PSC-derived endodermal precursors via the technique of directed differentiation. Thyroid progenitors derived in this way can be sorted to purity using lineage-selective fluorochrome reporters for further culture expansion and subsequent maturation. During maturation in 3D culture, the resulting cells form thyroid follicular organoids with an organized monolayered epithelium consistent with thyroid follicles, express genes required for hormone biosynthesis, and can function in vivo following transplantation into hypothyroid mice. Thus we have developed an in vitro system able to reveal the basic developmental mechanisms and gene programs of thyroid cells at early stages of embryonic development, and we have produced an inexhaustible source of sortable cells with structural and functional thyroid follicular capacity.

RESULTS

Nkx2-1⁺ Thyroid Cells Are Specified from ESC-Derived Endodermal Precursors upon Stimulation with Exogenous BMP4 and FGF2

We previously developed a directed differentiation protocol to produce ESC-derived definitive endodermal cells competent to form thyroid and lung epithelial lineages (Longmire et al., 2012). We employed an ESC line (Nkx2-1^{GFP}) carrying a knockin GFP reporter cDNA targeted to the locus encoding the homeodomain-containing transcription factor Nkx2-1, an essential regulator of thyroid and lung development. Within endoderm, Nkx2-1 is expressed only in lung or thyroid epithelia and is the first known protein induced upon endodermal specification to lung or thyroid fates. Nkx2-1⁺ cells induced from ESC-derived endoderm using our published (Longmire et al., 2012) six-factor cocktail (WFKBE+2; Figure 1A) expressed thyroid epithelial-specific genes, such as thyroglobulin (Tg). However, these cells did not display full thyroid maturation, as the genes required for iodine metabolism and thyroid hormone biosynthesis were not robustly expressed (i.e., the sodium iodine symporter [Nis] and thyroid peroxidase [Tpo]) (Figure S1A and data not shown).

Microarray analysis of the global mRNA expression profiles of these ESC-derived Nkx2-1^{GFP+} endodermal progenitors (Figure 1A and Tables S1 and S2) revealed multiple active signaling pathways, including BMP, Wnt, epidermal growth factor, and

FGF signaling. Hence, to identify the essential factors for thyroid cell development, we performed sequential withdrawal of each individual factor from the WFKBE+2 cocktail. We found BMP4 and FGF2 to be indispensable for efficient Nkx2-1⁺ endodermal induction. An induction medium composed of BMP4, FGF2, and Wnt3a led to the maximum efficiency of Nkx2-1⁺ cell specification by day 14, and sorted Nkx2-1^{GFP+} cells at this time point, either with or without Wnt3a, were competent to subsequently express the thyroid differentiation markers Tg and Tsh-r (thyroid-stimulating hormone [TSH] receptor) and the maturation markers Nis and Tpo (Figures 1B and S1A). Therefore, BMP4 and FGF2 are sufficient to specify endodermal cells in vitro toward Nkx2-1⁺ endodermal progenitor cells with thyroid potential.

Nkx2-1 Haploinsufficiency Affects the Differentiation of Thyroid Epithelial Cells, but Not the Efficiency of Nkx2-1⁺ Endodermal Lineage Specification

Because the Nkx2-1^{GFP} knockin reporter in our engineered ESCs replaced one Nkx2-1 allele, potentially creating haploinsufficiency (Figure 1C), we sought to test the effects of Nkx2-1 gene dosage on thyroid differentiation in vitro. We compared the Nkx2-1^{GFP} ESC line with a non-haploinsufficient Nkx2-1^{mCherry} ESC line where the mCherry fluorophore is knocked in 3' to the coding sequence (Bilodeau et al., 2014) (Figure 1C). The two lines were differentiated in parallel, and Nkx2-1^{GFP+} or Nkx2-1^{mCherry+} cells were sorted to purity on day 14 (Figure 1D), at which time the expression of Nkx2-1 mRNA was approximately 50% lower in the haploinsufficient Nkx2-1^{GFP+} cells than in the non-haploinsufficient Nkx2-1^{mCherry+} cells (Figure 1E). The expression of both early (Pax8) and all mature thyroid markers analyzed (Tg, Tsh-r, Nis, and Tpo) in the outgrowth of sorted Nkx2-1⁺ cells was diminished in Nkx2-1 haploinsufficient cells (Figure 1E). This was confirmed when the Nkx2-1^{GFP} line was compared with its parental syngeneic, non-haploinsufficient clone (Figure S1C). In contrast, we did not detect any difference in the rates of lineage specification of Nkx2-1⁺ endodermal cells on day 14, comparing haploinsufficient with normal ESC lines. The percentages and cell numbers of Nkx2-1⁺ cells specified by day 14 were similar in the Nkx2-1^{GFP} line and its parental clone (Figure S1B), as well as in the Nkx2-1^{mCherry} line (data not shown). Thus, Nkx2-1 haploinsufficiency does not affect specification of Nkx2-1⁺ endodermal cells but does affect subsequent maturation of thyroid epithelial cells. This is supported by observations in mice and humans who have Nkx2-1 haploinsufficiency and hypothyroidism (Krude et al., 2002).

The Expression of Pax8 Distinguishes a Subpopulation within Nkx2-1⁺ Endodermal Cells with Thyroid Potential

Having established a protocol able to produce putative thyroid follicular cells, next we sought to determine whether thyroid and lung lineage specification occurred in distinct endodermal Nkx2-1⁺ precursors, as is thought to occur in vivo. The Pax8 transcription factor is co-expressed with Nkx2-1 only in thyroid

(D) Representative sort gate on day 14 used to sort Nkx2-1^{mCherry+} cells specified with WB+2.

(E) mRNA expression by real-time RT-PCR comparing the Nkx2-1^{GFP} and Nkx2-1^{mCherry} ESC lines. The bars indicate fold change in gene expression over day 0 ESCs \pm SEM $2^{(-\Delta\Delta CT)}$; n = 2 independent experiments).

See also Figure S1 and Tables S1 and S2.

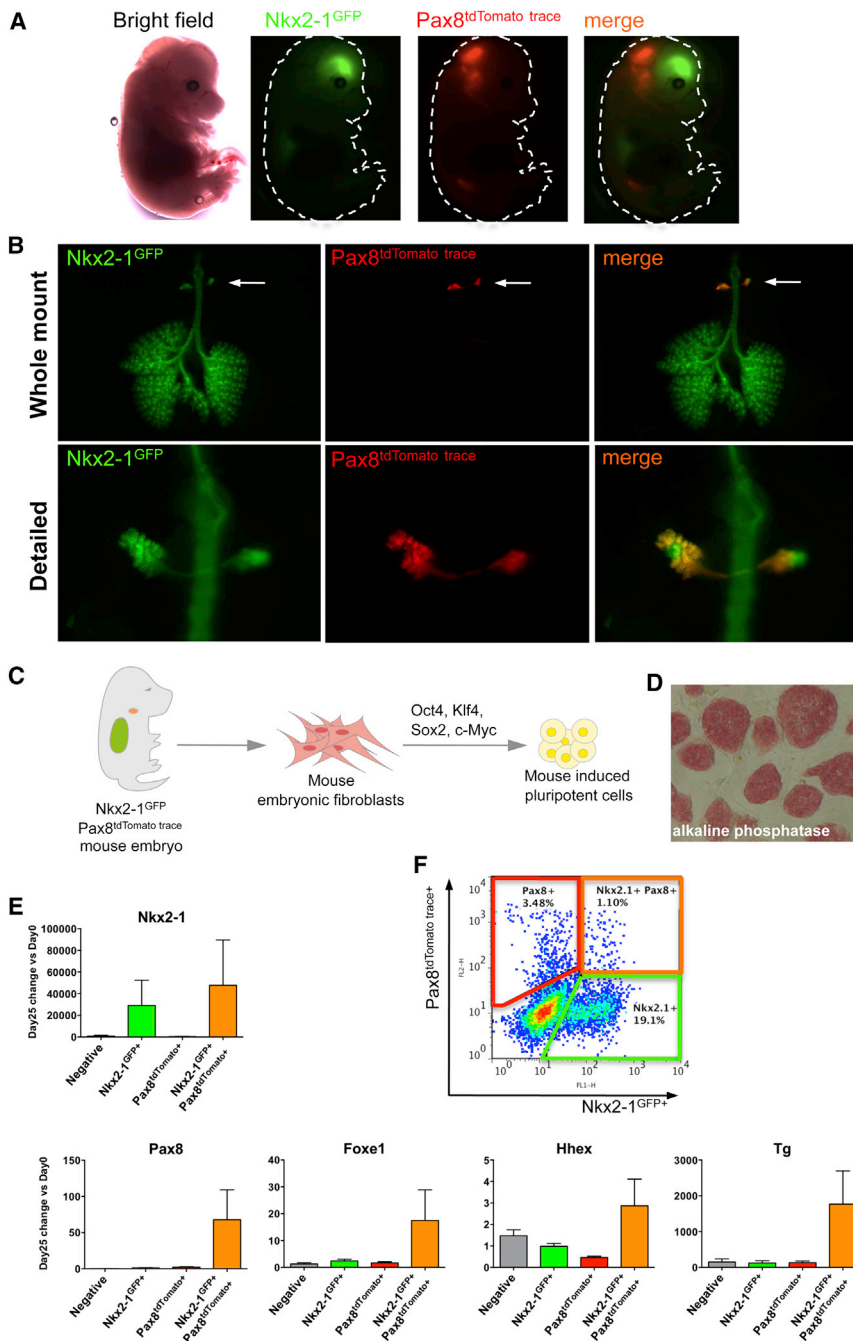


Figure 2. Thyroid Lineage Specification in Developing Embryos and in iPSC-Derived Endodermal Precursors Is Restricted to Cells Co-expressing Nkx2-1 and Pax8

(A) Representative E14.5 mouse embryo carrying Nkx2-1^{GFP} (forebrain and lung) and Pax8^{tdTomato} trace (midbrain, hindbrain, inner ear, and kidney) reporters.

(B) Dissection of E14.5 mouse embryo anterior foregut showing the developing lung and thyroid (arrow), with Nkx2-1^{GFP} and Pax8^{tdTomato} trace signal overlapping (merge) in the thyroid but not the lung. Note spherical Nkx2-1⁺/Pax8⁻ ultimobranchial bodies adjacent to each of the two Nkx2-1⁺/Pax8⁺ thyroid lobes.

(C) Schematic of iPSC derivation from MEFs by lentiviral-mediated transduction of the STEMCCA vector.

(D) Representative image of the resulting iPSCs, stained for the pluripotency marker alkaline phosphatase.

(E) Comparison of the four different sorted populations from (F). Cells were purified on day 14 using the gate indicated and replated for differentiation until day 25 (fold change mRNA expression on day 25 over day 0 by RT-qPCR; 2^[-ΔΔCT]). The bars indicate average fold change in gene expression over ESCs ± SEM (n = 3 independent clones).

(F) Representative FACS plot on day 14 of differentiation of the iPSC line from (C) and (D).

See also Figure S2.

Nkx2-1^{GFP}; Pax8^{tdTomato} trace) co-expressed both GFP and tdTomato reporters only in the thyroid epithelium, whereas GFP without tdTomato was expressed throughout the developing respiratory epithelium (Figures 2A and 2B). As previously reported, GFP was also expressed within developing ectoderm in the ventral forebrain (Longmire et al., 2012), and tdTomato without GFP was expressed in tissues known to express Pax8, including the kidney, hindbrain, midbrain, and inner ear (Figure S2A and as published [Bouchard et al., 2004]). We derived induced PSC (iPSC) clones carrying Nkx2-1^{GFP}; Pax8^{tdTomato} trace reporters by reprogramming mouse embryonic fibroblasts (MEFs) isolated from the bifluorescent mouse (Figures 2C, 2D, and S2B) and differentiated six lines in vitro using our Wnt3a, BMP4, and FGF2 Nkx2-1 induction protocol (Figures 2E and 2F). By day 14, all clones exhibited induction of the Nkx2-1^{GFP} reporter, with kinetics and efficiency similar to our previous report (Longmire et al., 2012), and Pax8^{tdTomato} trace⁺ cells represented 4.9% (±4.7) of all Nkx2-1⁺ cells. On the basis of GFP and tdTomato expression, we sorted four distinguishable populations on day 14 (Figure 2F) and further differentiated each population until day 25 (Figures 2E and S2C). Analysis of cells at the time of sorting (day 14) as well as until the full 25 days of differentiation of three clones revealed that only

epithelial cells, beginning at mouse E8.5 and human E20 in the foregut endoderm within the region of the prospective thyroid primordium (Fagman and Nilsson, 2010; Trueba et al., 2005). In contrast, Pax8 is not expressed at any developmental stage in lung epithelial cells. Hence, we developed a bifluorescent reporter system to track thyroid and non-thyroid fates in Nkx2-1⁺ cells by breeding mice with the GFP reporter targeted to the Nkx2-1 locus (Nkx2-1^{GFP}; Longmire et al., 2012), the Cre recombinase targeted to the Pax8 locus (Pax8^{Cre}; Bouchard et al., 2004), and a conditional Rosa26 tdTomato reporter (lox-stop-lox-tdTomato). As expected, these mice (hereafter Nkx2-

epithelial cells, beginning at mouse E8.5 and human E20 in the foregut endoderm within the region of the prospective thyroid primordium (Fagman and Nilsson, 2010; Trueba et al., 2005). In contrast, Pax8 is not expressed at any developmental stage in lung epithelial cells. Hence, we developed a bifluorescent reporter system to track thyroid and non-thyroid fates in Nkx2-1⁺ cells by breeding mice with the GFP reporter targeted to the Nkx2-1 locus (Nkx2-1^{GFP}; Longmire et al., 2012), the Cre recombinase targeted to the Pax8 locus (Pax8^{Cre}; Bouchard et al., 2004), and a conditional Rosa26 tdTomato reporter (lox-stop-lox-tdTomato). As expected, these mice (hereafter Nkx2-

the day 14 sorted GFP⁺ tdTomato⁺ population gave rise to cells expressing the constellation of four transcription factors (Parlato et al., 2004) that together uniquely identifies thyroid epithelia (Nkx2-1, Pax8, Foxe1, and Hhex) and the differentiation marker Tg (Figure 2E). In contrast, this population was depleted of cells competent to express the differentiated lung marker genes *Sftpc* and *Scgb1a1* (data not shown). In separate experiments using ESC lines that lack Pax8 reporters, we used fluorescence-activated cell sorting (FACS) analyses of intracellular protein to verify that Pax8 protein is expressed in approximately 5% of Nkx2-1⁺ ESC-derived cells (data not shown). We conclude that, as in the developing embryo, the thyroid lineage is specified in a distinct Nkx2-1⁺ endodermal population.

BMP and FGF Signaling Is Necessary and Sufficient for Thyroid Lineage Specification from Mouse and *Xenopus* Anterior Foregut Endoderm or ESC-Derived Definitive Endoderm

Having demonstrated that Pax8⁺/Nkx2-1⁺ thyroid progenitors were induced from PSC-derived endoderm by addition of Wnt3a, BMP4, and FGF2 (WB+2), we next sought to determine whether each pathway was necessary for thyroid lineage specification. In keeping with prior publications suggesting that Wnt is not required for thyroid specification from endoderm in vivo (Goss et al., 2009), we found that Nkx2-1^{GFP+} cells (Figure S1A) or Nkx2-1^{mCherry+} cells (Figure S3A) derived with BMP4 and FGF2 induction media (days 6–14) in the absence of Wnt3a displayed undiminished subsequent expression of thyroid markers after outgrowth. Although either BMP4 or FGF2 alone induced small numbers of Nkx2-1⁺ cells with little thyroid competence (Figures 3A and 3B), combinatorial use of BMP4 and FGF2 induced the highest percentage of thyroid competent Nkx2-1⁺ progenitors, as evidenced by subsequent robust expression of all early and mature thyroid markers, including Pax8, Tg, Tsh-r, Tpo, and Nis (Figures 3B and S3A). Consistent with these results, withdrawal of Wnt3a and/or addition of Wnt inhibitors Dkk1 or XAV-939 had no significant impact on the efficiency of lineage specification of Nkx2-1^{GFP+};Pax8^{tdTomato trace+} iPSC-derived cells by day 14, whereas there was a significant decrease in the percentage yield of GFP+/tdTomato+ cells when either BMP or FGF2 was removed from the Nkx2-1 induction media (data not shown).

To determine which downstream BMP and FGF signaling cascades are required for induction of thyroid fate, we supplemented the BMP4 + FGF2 media with specific inhibitors of either SMAD-dependent BMP signaling (Dorsomorphin), MEK1/2-dependent FGF or BMP signaling (PD98059; hereafter PD), PI3 kinase (PI3K)-dependent FGF signaling (LY294002; hereafter LY), or p38-MAPK-dependent BMP signaling (SB203580). We found reduced numbers and percentages of Nkx2-1⁺ cells in conditions supplemented with Dorsomorphin or LY (Figure 3C). Furthermore, when the rare Nkx2-1⁺ cells that were induced in the presence of these inhibitors were sorted to purity on day 14 and cultured further to allow completion of the protocol (without inhibitors), the progeny of these Nkx2-1⁺ cells showed reduced capacity to express mature thyroid markers, such as Tg and Tpo (Figure 3D).

Taken together, our findings in the ESC/iPSC in vitro model system suggested that canonical Wnt signaling may be dispens-

able for thyroid lineage specification, while combinatorial SMAD-dependent BMP signaling together with FGF signaling is required. To test this hypothesis in primary cells of the developing embryo, we used both the murine and *Xenopus* models of embryonic foregut organogenesis (Figures 4 and S4). First, in developing *Xenopus* embryos, we found evidence in support of active BMP and FGF signaling in the region of the thyroid primordium by immunostaining embryos for nuclear phospho-SMAD1/5/8, nuclear phospho-ERK1/2, and phospho-AKT ser473 proteins during early thyroid specification (Figure S4A). These phosphorylated signaling effectors were present in the foregut epithelium prior to and during the evagination of Nkx2-1⁺ cells of the developing thyroid anlage as well as in the surrounding mesenchyme (Figure S4A; stages NF20 and NF33).

Next, to assess whether FGF and BMP signaling is required for thyroid specification in vivo, we incubated developing mouse as well as *Xenopus* embryos in inhibitors of BMP or FGF signaling (Figures 4 and S4). Developing mouse foreguts were isolated by dissection at 6–8 somite stage (ss) (~E8.0) prior to detectable Nkx2-1 expression in the thyroid field and incubated for 2 or 3 days with the BMP inhibitor DMH-1. DMH-1 caused a marked reduction in phosphorylation of SMAD1/5 (Figure 4A, right, western blot) and blocked induction of both Nkx2-1 and Pax8 in the region of the mouse endodermal thyroid primordium (Figure 4A, left). Similarly, we incubated developing *Xenopus* embryos in inhibitors of BMP signaling (DMH-1 or an injected dominant-negative BMPR) or FGF signaling (SU5402, PD161570, or an injected dominant-negative FGFR), starting just after gastrulation (stage NF13) until stage NF20 (6–7 ss). The inhibitors were then removed and embryos allowed to develop until stage NF34 (36 ss), a time by which thyroid and lung lineages are normally specified (Shifley et al., 2012). In situ hybridization for markers of pharyngeal endoderm and thyroid lineage specification *foxe1*, *nkx2-1*, *pax2*, and *hhex* revealed that inhibition of either BMP or FGF signaling abrogated induction of all four thyroid markers in the vast majority of *Xenopus* embryos (Figures 4B and S4B). Furthermore, inhibition of PI3K-AKT with LY also prevented thyroid specification (Figure S4B). Immunostaining of pSmad1/5/8, pERK, and pAKT confirmed the efficacy of the inhibitors (Figure S4C). In contrast, when *Xenopus* embryos were incubated from stage NF13 through NF35 in inhibitors of canonical Wnt signaling (XAV939), RA signaling (BMS493), or VEGF signaling (KRN633), we observed normal *nkx2-1* induction in the thyroid primordium (Figure S4B), indicating that Wnt, RA, and VEGF signaling at these developmental stages is dispensable for thyroid specification.

To assess the stage dependence of these signaling requirements, we varied the timing of BMP and FGF loss of function during foregut endoderm development. We observed that early inhibition of BMP or FGF signaling beginning at stage NF13 (analogous to mouse E7.5) blocked induction of *nkx2-1* (Figure S4B), whereas inhibition beginning later (at stage NF20; Figure S4D) did not, suggesting that the requirement for BMP and FGF signaling in thyroid lineage specification is restricted to a narrow developmental window between stages NF13–20.

Because our mouse ESC model had predicted that FGF2 and BMP4 were sufficient to induce thyroid lineage specification, we next asked whether exogenous FGF2 and BMP4 were sufficient

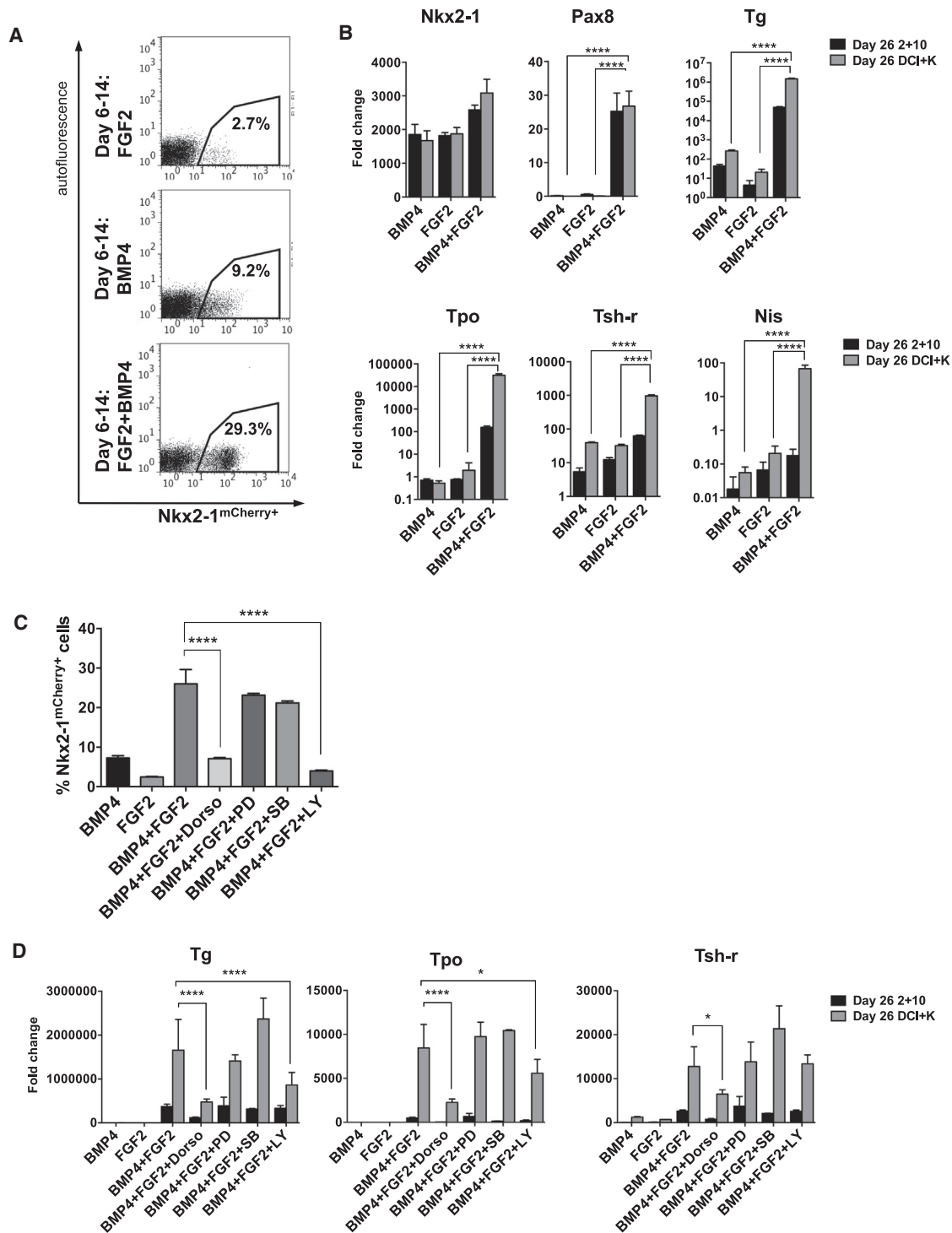


Figure 3. BMP and FGF Signaling Is Necessary for Thyroid Lineage Specification of ESC-Derived Definitive Endoderm

(A) Representative gates used to sort Nkx2-1^{mCherry+} cells specified with only FGF2, only BMP4, or FGF2+BMP4 on day 14.

(B) Fold change of mRNA expression on day 26 over day 0 by RT-qPCR; $2^{(-\Delta\Delta CT)}$. Cells were purified on day 14 using the gate indicated in (A) and replated for differentiation until day 26.

(C) Quantitation by flow cytometry of the percentage of Nkx2-1^{mCherry+} cells specified on day 14 using different specification media (days 6–14) containing 4 μ M of Dorsomorphin, 20 μ M of PD, 10 μ M of SB203580 (SB), or 25 μ M of LY. The error bars indicate mean \pm SD (n = 3 biological replicates).

(D) mRNA expression on day 26 of the Nkx2-1^{mCherry} ESC line, comparing the specification media used in (C). Bars indicate average fold change in gene expression ($2^{(-\Delta\Delta CT)}$) over day 0 ESCs \pm SD (n = 3 biological replicates). Two-way ANOVA (a and c) and one-way ANOVA (b); *p \leq 0.05, ****p \leq 0.0001.

See Figure S3.

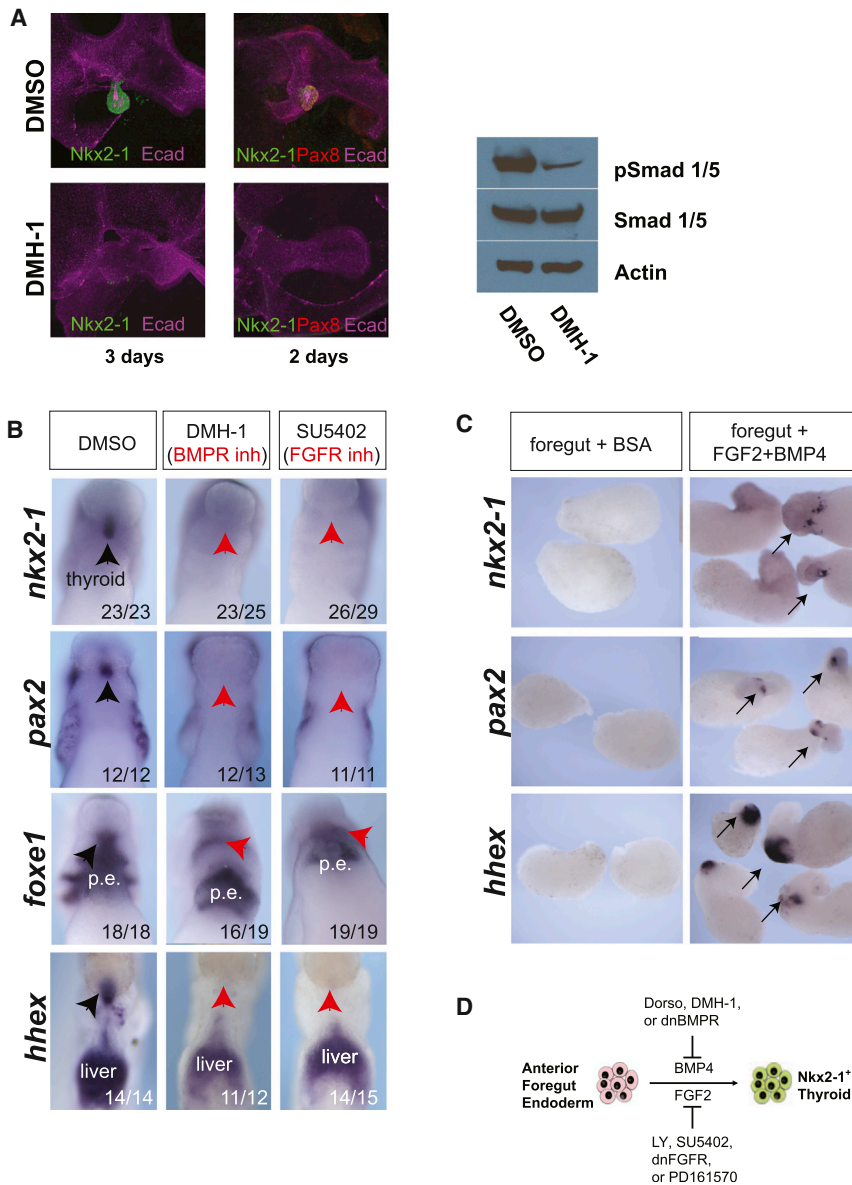


Figure 4. ESC Models Predict the Evolutionarily Conserved Pathways That Are Necessary and Sufficient for Thyroid Specification in Mouse and *Xenopus* Embryos

(A) BMP signaling blockade abrogates thyroid bud formation in mouse: whole foreguts from E8.0 embryos (6–8 ss) were cultured for 2–3 days in the presence of the BMP antagonist DMH-1. Colocalization of Nkx2-1+ and Pax8+ shows a discrete thyroid bud formed in control cultures (upper left). No thyroid bud was apparent when BMP signaling was inhibited (lower left). Reduced pSmad1/5 content in the presence of DMH-1 (right; western blot).

(B) In vivo pharmacological loss of function using antagonists of type I BMP receptor (DMH-1) or FGF receptor (SU5402) activity in *Xenopus* embryos. Whole embryos were cultured in the presence of the antagonists from stage NF13–20 and assayed for the indicated genes at stage NF35. The number of embryos with the displayed phenotype is indicated.

(C) FGF and BMP signaling is sufficient to induce thyroid gene expression in dissected *Xenopus* foregut endoderm explants. Explants were dissected at stage NF15, cultured until NF35, and assayed for the indicated genes.

(D) Schematic of inhibition of BMP4 or FGF2 signaling blocking thyroid specification. See also Figure S4.

TSH and 3D Culture Promotes ESC-Derived Thyroid Follicular Maturation and Organoid Formation

Having interrogated the signals required for the induction of thyroid fate, next we focused on augmenting the maturation state of the thyroid epithelial progenitors generated from PSCs, using the Nkx2-1^{mCherry} ESCs. In contrast to lineage specification and early development, the expression of thyroid genes necessary for iodine metabolism, Nis and Tpo, is associated with later gland maturation

to induce thyroid development in *Xenopus* foregut endoderm (Figure 4C). Foregut explants were micro-dissected at stage NF15, prior to thyroid specification, and the mesoderm was removed. The foregut endoderm explants were then cultured until stage NF35 either without growth factors or with a combination of FGF2 and BMP4. In situ hybridization revealed that only explants incubated with FGF2 and BMP4 expressed *nkx2-1*, *pax2*, and *hhhex* (Figure 4C). We did not detect expression of *sftpc* in explants from sibling embryos (data not shown), suggesting that the *nkx2-1* expression was thyroid and not respiratory epithelium. Taken together, these results from *Xenopus* and mouse embryo models extended our observations made in differentiating mouse ESCs and iPSCs, confirming that FGF signaling and BMP signaling are evolutionarily conserved pathways required for the specification of thyroid fate from developing endoderm both in vitro and in vivo (Figure 4D).

(Figure 5A) and has been shown in vivo to require TSH receptor activation (Postiglione et al., 2002). Hence we tested the effect of TSH at various developmental stages of our in vitro protocol, either on induction of Nkx2-1⁺ progenitors (days 9–12) or during outgrowth of sorted Nkx2-1⁺ cells (days 14–22). We found that the addition of TSH prior to lineage specification (days 9–12) had no detectable effect on the efficiency of thyroid lineage specification or the competence of thyroid cells to subsequently differentiate (data not shown). In contrast, addition of TSH after lineage specification (days 14–22) resulted in increased Nis, Tsh-r, and Tpo expression (Figure S5A) but no significant change in the expression of lineage markers Nkx2-1 and Pax8 (data not shown). An additional 3 days of culture maturation in the presence of TSH was accompanied by further augmentation of Nis and Tsh-r expression (Figure S5A).

We previously published augmented thyroid gene expression in ESC-derived Nkx2-1⁺ cells when using a thyroid medium

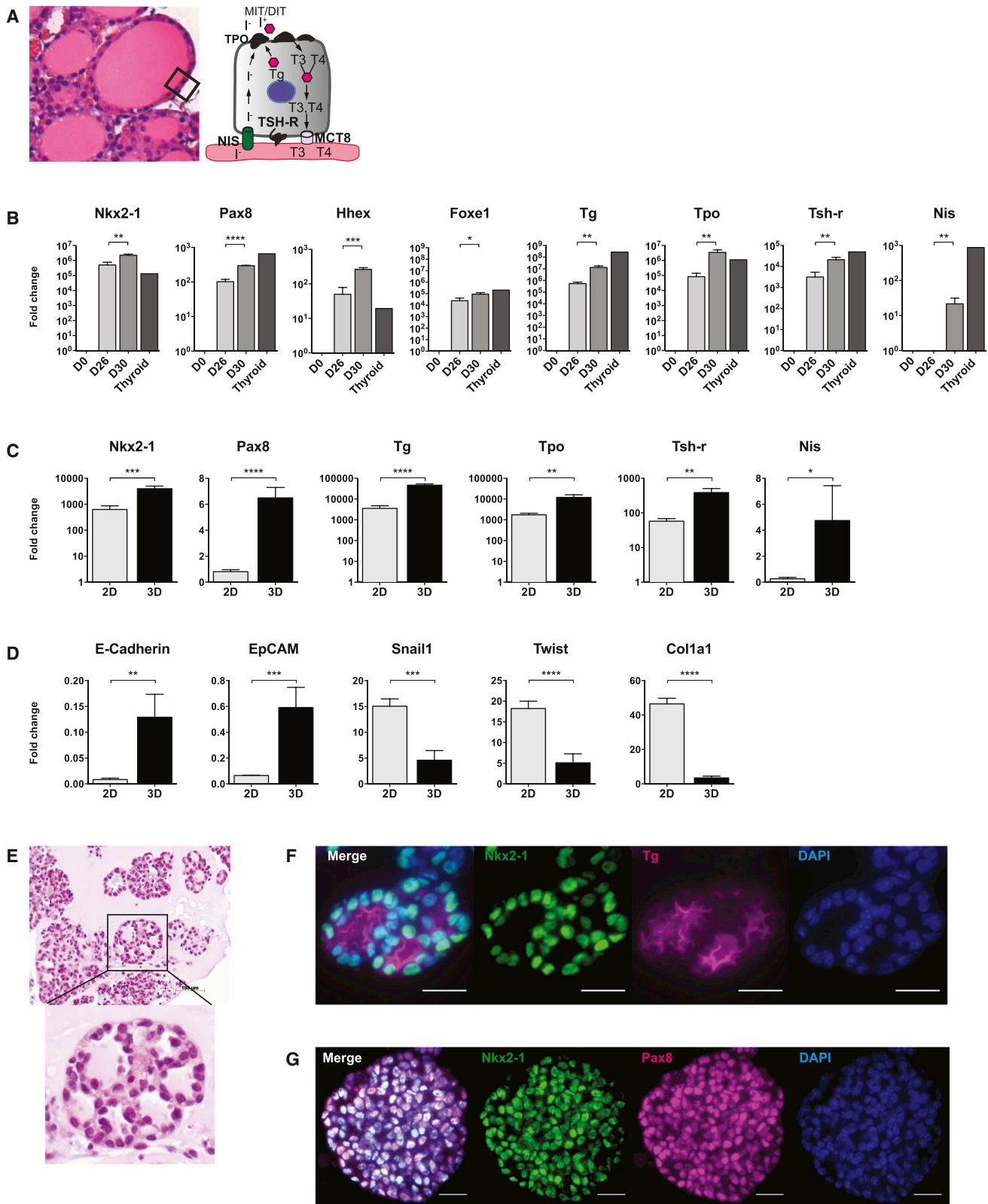


Figure 5. In Vitro Development of ESC-Derived Thyroid Follicular Cells by Directed Differentiation

(A) Hematoxylin and eosin (H&E) staining of sectioned mouse thyroid tissue (left) and schematic of a thyroid follicular cell (right).

(B) Effect of time in culture on thyroid marker gene expression comparing day 26 versus day 30.

(legend continued on next page)

containing IGF-1, insulin, transferrin, and selenium (Longmire et al., 2012). Therefore, we included these additives, together with TSH, in our prior base medium of FGF2 + FGF10. This “thyroid outgrowth medium” was used for replating the sorted Nkx2-1⁺ cells on day 12 (Figure S5B). For the final maturation stages after expansion of sorted cells in “thyroid outgrowth medium,” we sought to further optimize expression of Nis and Tpo. Because we had observed induction of these markers in response to either DCI+K (Figure 1E) or in response to 1–100 mU/ml of TSH (data not shown), we tested the effect of combinations of each of these factors (Figure S5C; days 22–26). We found that withdrawal of either cyclic AMP (cAMP) or dexamethasone from the DCI+K cocktail adversely affected maturation (Figure S5C); however, substitution of TSH for cAMP in the DCI+K medium retained maturation and resulted in the most robust expression of Nis (Figure S5C). Thus, the combination of dexamethasone and TSH was included in the final 4 days of maturation (days 26–30), resulting in the thyroid directed differentiation protocol summarized in Figure S5B and achieving the derivation from ESCs of a population of cells expressing thyroid marker transcripts at levels equal to (Nkx2-1, Hhex, Foxe1, Tpo) or within 10-fold of (Pax8, Tg, Tshr, Nis) post-natal murine thyroid control tissue (Figure 5B).

To facilitate thyroid follicular structural formation during outgrowth of ESC-derived Nkx2-1⁺ cells, based on prior reports of Matrigel as a favorable thyroid culture substrate (Martin et al., 1993), we tested the effect of 3D culture in Matrigel (days 12–30; Figures 5C and 5D). Compared with 2D culture, we found that culture of purified Nkx2-1^{mCherry+} cells in 3D Matrigel conditions resulted in higher expression of thyroid genes by qPCR (Nkx2-1, Pax8, Tg, Tshr, Tpo, and Nis; Figure 5C), increased epithelial gene expression (increased E-Cadherin and EpCam expression and reduced mesenchymal markers Snail1, Twist, and Col1a1; Figure 5D), and triggered the formation of follicular-like clusters of cells (Figure 5E). By day 30, we observed 130 ± 17 follicular clusters emerging from each 65,500 Nkx2-1^{mCherry+} cells plated on day 12 in a well of a 24-well plate. By day 30 in culture, 50% of the progeny of the Nkx2-1^{mCherry+} sorted cells expressed Pax8 protein by FACS, 46% expressed Tg, and 96% continued to express Nkx2-1 by either microscopy or FACS for the mCherry reporter (data not shown). Most important, phenotyping of the resulting clusters or organoids revealed them to have the 3D structure and molecular phenotype typical of thyroid follicles, including formation of organized monolayered Nkx2-1⁺ Pax8⁺ epithelia surrounding a lumen filled with Tg (Figures 5F and 5G). These organoids could be further passaged and maintained in these culture conditions with stable or increased expression of Nkx2-1, Pax8, Hhex, Foxe1, Tg, Nis, Tshr, and Tpo until at least day 52 (Figure S5D). In addition, after incubation in iodinated media for 48 hr, the organoids displayed the functional capacity to organify iodine and produce small amounts of T4 hormone bound to TG in vitro at different time

points during the differentiation protocol, beginning on day 30 (Figure S5E).

In Vivo Function of Purified ESC-Derived Thyroid Follicular Organoids following Transplantation into Hypothyroid Mouse Recipients

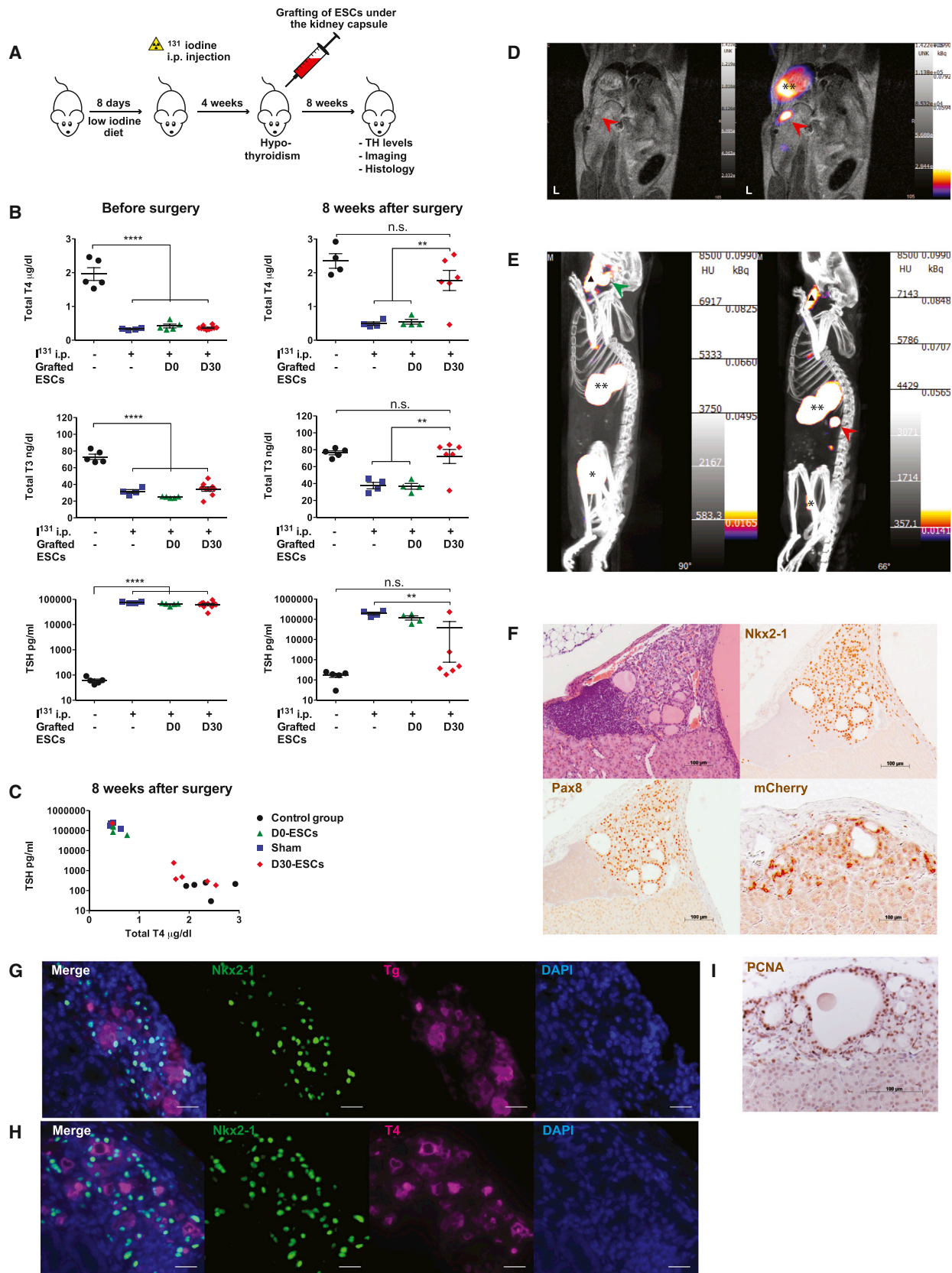
The defining functional characteristic of thyroid follicular epithelial cells is their capacity to synthesize and secrete thyroid hormones in vivo. Hence, we sought to test whether ESC-derived Nkx2-1^{mCherry+} thyroid progenitors sorted on day 12 of differentiation and further matured into organoids until day 30 could function in vivo after transplantation and moreover whether these cells could rescue hypothyroid mice. Syngeneic mouse recipients underwent radioiodine ablation of their native thyroid tissue after 8 days of a low-iodine diet in order to induce severe hypothyroidism, evident as significantly reduced circulating plasma T4 and T3 levels and elevated circulating TSH levels (Figures 6A and 6B). Four weeks later, we prepared one positive control mouse group (n = 5) that had not undergone radioiodine ablation, one negative control group that received sham surgery (n = 4), and two experimental recipient groups that received either undifferentiated ESCs (day 0 ESCs, hereafter “D0-ESCs”; n = 5) or differentiated ESCs that had been sorted on day 12 on the basis of Nkx2-1^{mCherry+} expression and further differentiated until day 30 in our complete 3D protocol (hereafter “D30-ESCs”; n = 10). Following ESC transplantation with 2.5–3 × 10⁶ cells beneath the left kidney capsule of each mouse recipient, we followed all recipient groups for at least 8 weeks post-transplantation, monitoring circulating T4, T3, and TSH levels, and we used both MRI and single-photon emission computed tomography (SPECT)/computed tomography (CT) to screen for in vivo graft growth and function (Figures 6 and S6).

Starting 2–4 weeks post-transplantation, recipients of D30-ESCs displayed augmented circulating T4 and T3 levels that continued to increase over time until they approached normal levels by 8 weeks after transplantation (Figures 6B, S6A, and S6C). Reconstitution of T4 levels was accompanied by amelioration of the elevated plasma TSH levels (Figures 6B, 6C, and S6B), further emphasizing that physiologic rescue was occurring. In a repeat experiment, some recipients followed for longer periods were observed to display circulating T4 reconstitution at normal levels for at least 29 weeks after transplantation (data not shown). In contrast, we observed no reconstitution of circulating thyroid hormone levels in either sham transplanted controls or recipients of D0-ESCs, excluding the possibility that either residual undifferentiated cells or re-growth of native thyroid tissue was responsible for the return of circulating T4 or the dampening of the TSH response.

To further evaluate the function of the transplanted cells, we incorporated imaging with sodium pertechnetate (Tc^{99m}) and SPECT/CT co-registered with MRI. Importantly, the uptake of Tc^{99m} into thyroid tissue is mediated by Nis, allowing its

(C and D) Comparison of 3D versus 2D culture on thyroid gene expression. (B–D) Bars indicate average fold change in gene expression by real-time RT-PCR over day 0 ESCs ± SD (n = 3 biological replicates, post-natal mouse thyroid tissue n = 1).

(E–G) Histology on day 30 of outgrowth and differentiation of Nkx2-1^{mCherry+} cells sorted on day 12 as H&E-stained paraffin sections (E). Immunofluorescence microscopy of day 30 ESC-derived follicular-like structures after immunostaining for Nkx2-1 and Tg (F), Nkx2-1, and Pax8 (G). Nuclei are counterstained with DAPI (E and G). The scale bars represent 100 μm (E) and 10 μm (F and G). *p ≤ 0.05, **p ≤ 0.01, ***p ≤ 0.001, and ****p ≤ 0.0001 (Student's t test). See also Figure S5.



(legend on next page)

visualization to be a surrogate for iodine uptake (Zuckier et al., 2004). In recipients of D30-ESCs, we observed Tc^{99M} uptake occurring in the region of the kidney capsule grafts (Figures 6D, 6E, and S6E). We also observed low levels of Tc^{99M} uptake in the large masses that derived from kidney capsule transplantation of D0-ESCs (Figure S6D), but in no D0-ESC recipient was this signal accompanied by detectable return of circulating T4 levels. As expected, Tc^{99M} uptake was not detected in the anatomical region of the native thyroid tissue of any ablated recipient (Figures 6E and S6E), further suggesting that return of thyroid function in D30-ESC recipients was not due to re-growth of native thyroid tissue.

To confirm the presence of engrafted D30-ESCs in vivo, we evaluated the histology of the renal lesions that had been visualized by MRI and SPECT (Figures 6F–6I). As expected, recipients of D0-ESCs developed large teratomas (Figure S6D) without evidence of organized follicles, and only rare, if any, cells expressed nuclear Nkx2-1 protein (data not shown). In contrast, no teratomas were observed in recipients of D30-ESCs; instead, these recipients displayed persistent grafted cells beneath their kidney capsules organized into many follicular-like structures per high power field that were morphologically consistent with thyroid epithelial follicles (Figure 6F). These structures consisted of mCherry⁺ epithelial cells expressing nuclear Nkx2-1 and Pax8 proteins by immunostaining, surrounding central lumens filled with colloid-like material that contained Tg and T4 (Figures 6F–6H). A subset of the grafted cells expressed the proliferation marker PCNA (Figure 6I). We did not detect expression of pro-Sftpc in any grafted cell suggesting that Nkx2-1 expression resulted from thyroid and not respiratory epithelium (Figure S6F).

To assess whether the engrafted D30-ESCs functioned in a regulated fashion, we exposed additional D30-ESC transplanted mice, negative sham controls, and positive normal controls (n = 5 per group) to a high dose of exogenous T3 expected to fully suppress endogenous TSH and hence T4 production. Indeed, in all groups, administration of T3 resulted in TSH suppression and abrogated T4 secretion (data not shown). To further interrogate TSH responsiveness (Figure S6G), we then injected each mouse with exogenous bovine TSH and 3 hr later observed an increase in circulating T4 in positive control mice as well as in recipients of D30-ESCs, but not in sham controls, consistent with the regulation of engrafted cells by TSH.

These results indicate that ESC-derived thyroid follicular epithelial cells prepared by directed differentiation in serum-

free, feeder-free conditions exhibit in vivo functional potential, including the capacity to rescue hypothyroid mice that otherwise lack native functional thyroid tissue.

Derivation of Human Thyroid Progenitors from ESCs and Hypothyroid Patient-Specific iPSCs

Finally, we sought to adapt our protocol to direct the differentiation of human ESCs and iPSCs into thyroid progenitors. Having observed that thyroid specification was not affected by Nkx2-1 haploinsufficiency in mouse PSCs (Figures 1 and S1), we hypothesized that BMP4 and FGF2 might also generate human thyroid progenitors in normal as well as haploinsufficient lines. Hence we obtained dermal fibroblasts from three hypothyroid children previously diagnosed with the brain-lung-thyroid syndrome arising from three different respective NKX2-1 coding sequence mutations (Figures S7A and S7B) that were predicted to cause NKX2-1 haploinsufficiency (Hamvas et al., 2013). Using the STEMCCA reprogramming system (Somers et al., 2010), we generated iPSC lines from each child's fibroblasts (hereafter T1, T3, and T4; Figures 7A, 7B, and S7C–S7E). Next, we derived definitive endoderm from each iPSC line as well as from control human ESCs (RUES2) and control iPSCs (BU3 and iPS17; Figure 7C and Supplemental Experimental Procedures). We used dual inhibition of TGF β and BMP signaling, as originally described by Green et al. (2011) in order to mimic anterior foregut patterning of each ESCs/iPSCs-derived endodermal population and then tested the capacity of varying concentrations of BMP4 and FGF2 to specify putative thyroid cells. Using the control RUES2 line, we varied the doses of BMP4 and FGF2 to identify a dosing combination that resulted in induction of clusters of NKX2-1+/PAX8+ co-expressing cells (Figures 7D and S7F). This same dose induced NKX2-1+/PAX8+ cell clusters from human iPSC lines BU3 and iPS17, as well as from all three patient-specific iPSC lines (Figure 7E, left, and Figure S7G). BMP4 or FGF2 alone induced rare, if any, NKX2-1+/PAX8+ co-expressing cells in the T1, T3, T4, and RUES2 lines (data not shown). Furthermore, in BU3, iPS17, and T3 iPSC-derived endodermal cells subjected in parallel to published lung inducing medium (Huang et al., 2014) that contains BMP4 (with Chir, FGF10, FGF7, and RA [CFKBRA]) but lacks FGF2, we observed only induction of NKX2-1+ cells without co-expression of PAX8, suggesting that these cells were respiratory rather than thyroid (Figure 7E, right). As in our mouse ESC/iPSC experiments, NKX2-1+/PAX8+, putative thyroid progenitors induced after

Figure 6. In Vivo Function of Transplanted ESC-Derived Putative Thyroid Follicles in Hypothyroid Mice

(A) Experiment overview for generation of hypothyroid mice and rescue with in vitro-derived thyroid follicular cells.

(B) Recovery of circulating total T4, T3, and TSH 8 weeks after transplantation of thyroid follicular-like cells derived from ESCs (D30-ESCs) but not undifferentiated ESCs (D0-ESCs). Data indicate each individual mouse plasma level (dots, squares, and triangles) as well as mean \pm SEM for each group. **p \leq 0.01 and ****p \leq 0.0001 (one-way ANOVA). Over the time course shown, four mice in the D30-ESCs group died.

(C) Circulating TSH plotted versus T4 for individual recipients 8 weeks after surgery.

(D) Eight weeks after transplantation, MRI shows a mass (red arrow) on the left kidney (left); SPECT co-registered with MRI shows overlay with the mass (red arrow, right).

(E) Tc^{99M} SPECT/CT shows signal in the anatomical region of the native thyroid gland (green arrow) in a positive control mouse (left) and a hot spot (red arrow) on the left kidney in a D30-ESC recipient (right) 8 weeks after surgery but no signal of the native thyroid tissue in the ablated mouse (right). Tc^{99M} uptake in bladder (*), stomach (**), and submandibular gland (black triangle).

(F–I) Kidney tissue sections 8 weeks after transplantation of D30-ESCs. (F) H&E staining of transplanted cells in the host kidney expressing nuclear Nkx2-1, nuclear Pax8, and mCherry. (G and H) Immunostaining for Nkx2-1 and Tg (G) or Nkx2-1 and T4 (H). PCNA immunohistochemistry of day 30 ESC-derived cells (I). Nuclei are counterstained with DAPI (G and H) or H&E (I). The scale bars represent 100 μ m (F and I) and 10 μ m (G and H).

See also Figure S6.

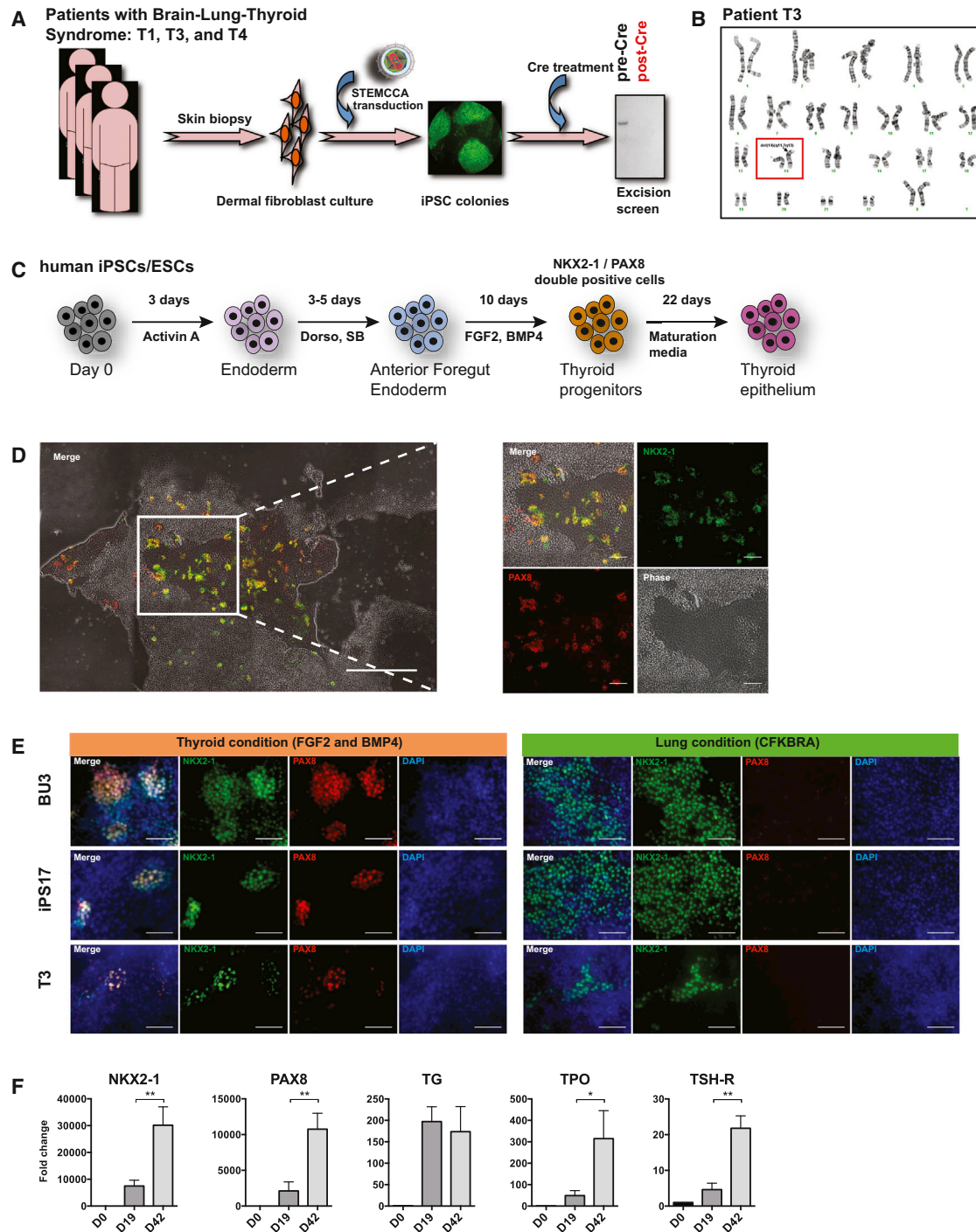


Figure 7. Derivation of Human Thyroid Progenitors from Human ESCs/iPSCs and Hypothyroid Patient-Specific iPSCs

(A) Reprogramming strategy to generate iPSCs lines from a cohort of three children with brain-lung-thyroid syndrome. Dermal fibroblasts were reprogrammed with the hSTEMCCA-loxP lentivirus, and clones were screened for a single integrated STEMCCA copy, which was then excised by transient Cre recombinase. (B) Karyotype of patient T3 (clone T3-2Cr3) indicates the known disease-causing deletion of the NKX2-1 locus (red box): interstitial deletion on chromosome 14 between bands q11.2 and q13.

(C) Schematic of directed differentiation protocol of human iPSCs/ESCs into thyroid progenitors.

(D) Immunofluorescence microscopy on day 19 of differentiation of RUES2-derived NKX2-1+/PAX8+ clusters. Overview (left; the scale bar represents 500 μ m) and zoom (right; the scale bars represent 50 μ m).

(legend continued on next page)

10 days of exposure to BMP4 and FGF2 expressed low to undetectable levels of TPO and TSH-R transcripts (data not shown). However, after further culture in the same thyroid differentiation and maturation conditions used for mouse ESCs, these thyroid differentiation markers were upregulated, and NKX2-1, PAX8, and TG expression was maintained for at least 42 days in culture (Figure 7F). As expected, without the use of a human NKX2-1 reporter for purification of human thyroid cells from these heterogeneous endodermal cultures, these thyroid markers were detected at significantly lower levels than adult human thyroid control tissue biopsies (data not shown). Taken together, these findings support the capacity of combinatorial BMP and FGF signaling to induce thyroid lineage specification from developing endoderm across species, from *Xenopus* to mice to humans, and enable the generation of patient-specific thyroid progenitors from individuals with genetic or congenital hypothyroidism.

DISCUSSION

Two applications of in vitro model systems, deriving from ESCs and iPSCs, are frequently touted: (1) the engineering of cell-based therapies able to durably ameliorate disease or regenerate tissue after a single transplantation treatment and (2) the production of an inexhaustible supply of purified cells of defined lineage at identifiable developmental stages for basic mechanistic studies. Here we demonstrate the application of ESCs and iPSCs toward both goals. We have used these cells to produce functional, transplantable thyroid follicular organoids able to produce circulating thyroid hormone in vivo at levels that rescue hypothyroid mice, and we have produced thyroid precursor cells at an early developmental stage, revealing that combinatorial BMP signaling and FGF signaling together are required for thyroid lineage specification from multi-potent definitive endoderm.

Although ESC/iPSC model systems frequently have been used to confirm or validate developmental signaling pathways identified in vivo or in explants, we used ESCs and iPSCs to discern a novel role for combinatorial BMP and FGF signaling in thyroid lineage specification, and argue against a role for any individual signaling pathway in isolation. Our findings agree with previous work suggesting a role for FGF signaling in early thyroid development. Our finding of nuclear pERK1/2 protein staining in endodermal Nkx2-1⁺ thyroid progenitors in *Xenopus* embryos is consistent with prior demonstrations of active FGF signaling in the developing *Xenopus* ventral foregut endoderm (Shifley et al., 2012). Moreover, a role for FGF signaling in inducing thyroid cell fate has been previously demonstrated in mouse endodermal explant studies, in which the addition of exogenous FGF2 prior to thyroid specification induced Nkx2-1 and Tg (Serls et al., 2005). In zebrafish models inhibition of FGF prior to specification leads to absence of a thyroid primordium (Wendl et al., 2007), and mouse genetic models establish that FGF signaling is required for normal early thyroid develop-

ment, with the adjacent cardiac mesoderm likely being the source of this signal (Celli et al., 1998; Fagman et al., 2007; Fagman and Nilsson, 2010; Kameda et al., 2009; Lania et al., 2009; Vitelli et al., 2002).

In contrast, only two prior studies, featuring Chordin mutant and Twisted mutant mice with perturbed BMP signaling, have reported thyroid hypoplasia, raising the possibility of a role for BMP signaling in thyroid development (Bachiller et al., 2003; Petryk et al., 2004). These prior reports could not discern whether the thyroid defects were primary effects due to inhibition of lineage specification, reduced proliferation, or secondary effects due to perturbed cardiac field development. We used our PSC model system, confirmatory *Xenopus* embryos, and mouse developing foregut endoderm explant models to interrogate the period of thyroid lineage specification from endoderm. We observed that the BMP signal transducers phospho-SMAD1/5/8 are present in the nuclei of endodermal thyroid progenitors at the time of lineage specification, and SMAD-dependent BMP signaling is necessary for induction of the Nkx2-1⁺ thyroid program. The precise mechanisms by which BMP signaling induces thyroid fate warrants further study to determine whether these are similar to those that induce endodermal Nkx2-1⁺ lung progenitors.

Identification of the sequence of developmental signals that promote thyroid development from endoderm allowed us to perform the generation of functional thyroid follicular-like epithelial cells by the technique of “directed differentiation” of PSCs. In accordance with prior observations from mouse genetic models (Postiglione et al., 2002), we observed TSH signaling to be dispensable for early thyroid specification; however, TSH promoted the maturation of the genetic program necessary for hormone synthesis. As suggested by observations made in patients with hypothyroidism due to NKX2-1 haploinsufficiency (Krude et al., 2002), we also found thyroid differentiation subsequent to lineage specification to be profoundly sensitive to Nkx2-1 haploinsufficiency in our in vitro mouse model system. Furthermore, we were able to apply our protocol to successfully generate NKX2-1⁺/PAX8⁺ human thyroid progenitors in iPSCs generated from patients with brain-lung-thyroid disease presenting with hypothyroidism. However, these double positive clusters were rare events, possibly because of the NKX2-1 haploinsufficiency that causes the syndrome.

Because the defining feature of thyroid follicular epithelial cells is functional hormone biosynthesis, our transplantation studies provided an important functional assessment of the thyroid organoids we generated by directed differentiation. After transplantation beneath the kidney capsules of hypothyroid mouse recipients, we found evidence for durable, functional engraftment of the putative organoids, which after 8 weeks in vivo (1) retained recognizable structure, (2) continued to express the molecular phenotype of thyroid follicular epithelia, (3) produced circulating T4 and T3, and (4) were regulated by TSH. To prove that these grafted organoids derived from Nkx2-1⁺ endodermal precursors, an important aspect of our work involved the sorting

(E) Immunostaining for NKX2-1 and PAX8 on day 17 of differentiation in multiple human iPSC lines in either thyroid or lung specification medium. Nuclei are counterstained with DAPI. The scale bars represent 50 μ m.

(F) mRNA expression of thyroid marker genes. The bars indicate average fold change over undifferentiated iPSC17 mean \pm SD (n = 3 biological replicates). *p \leq 0.05 and **p \leq 0.01 (Student's t test).

See also Figure S7.

to purity of only Nkx2-1^{mCherry+} endodermal cells prior to transplantation. This sorting algorithm should also help minimize the chance of teratomas developing in vivo from any residual undifferentiated cells. Indeed, no teratomas were observed arising from the sorted, transplanted cells in any recipient in our studies.

In summary, we present a novel in vitro model system based on the directed differentiation of PSCs into thyroid progenitors and mature follicular epithelial organoids for basic developmental studies and in vivo functional thyroid tissue regeneration. This system recapitulates the developmental milestones of early thyroid development, revealing previously unknown mechanisms of thyroid organogenesis. Successful functional transplantation of the resulting cells also suggests the feasibility of a potential future cell-based therapy for hypothyroidism.

EXPERIMENTAL PROCEDURES

Experimental methods are further detailed in the [Supplemental Information](#) and in downloadable protocols posted online at <http://www.bumc.bu.edu/stemcells>.

Animal Maintenance

All studies involving mice carrying GFP and tdTomato reporters were approved by the Institutional Animal Care and Use Committee of Boston University School of Medicine. All murine transplantation experiments were approved by the Beth Israel Deaconess Medical Center Institutional Animal Care and Use Committee.

Mouse ESC and iPSC Lines

Derivation of the Nkx2-1^{GFP} and Nkx2-1^{mCherry} knockin reporter ESC lines by homologous recombination was previously published and is further detailed in the [Supplemental Information](#) (Bilodeau et al., 2014; Longmire et al., 2012). The Nkx2-1^{GFP};Pax8^{tdTomato trace} iPSC reporter line was generated by transduction of MEFs with the dox-inducible Tet-STEMCCA reprogramming lentiviral vector. All ESCs and iPSCs were maintained on fibroblast feeder layers using serum-containing media and LIF (ESGRO Chemicon).

Mouse ESC/iPSC Directed Differentiation

Cell differentiation was performed in complete serum-free differentiation medium (cSFDM; see [Supplemental Experimental Procedures](#)) supplemented with the indicated factors. Briefly, definitive endoderm was induced in embryoid body suspension cultures with 50 ng/ml Activin A (R&D), as previously published (Longmire et al., 2012). Next, 100 ng/ml mNoggin (R&D) and 10 μ M SB431542 (Sigma) was applied for 24 hr to generate anterior foregut endoderm. Expression of Nkx2-1 was induced with specification medium containing 100 ng/ml mWnt3a, 10 ng/ml mKGF, 10 ng/ml hFGF10, 10 ng/ml mBMP4, 20 ng/ml hEGF, and 250 ng/ml mFGF2 (all from R&D). After Nkx2-1 induction, cells were sorted on days 12–14 by flow cytometry on the basis of expression of GFP, mCherry, or tdTomato reporters and then replated for either 2D or 3D culture outgrowth as indicated. For 2D outgrowth, plated cells were grown in gelatin-coated dishes for 8 more days in cSFDM with 250 ng/ml mFGF2, 100 ng/ml hFGF10, and 100 ng/ml heparin sodium salt. On day 22, the medium was switched to DCI+K maturation medium (see [Supplemental Experimental Procedures](#)). For 3D outgrowth, cells were plated in pure growth factor reduced Matrigel drops (Corning) in cSFDM supplemented with 250 ng/ml mFGF2, 100 ng/ml hFGF10, 50 ng/ml mIGF-1, 25 ng/ml hEGF (all from R&D), 100 ng/ml heparin sodium salt, 10 μ g/ml insulin (Sigma), and 1 mU/ml bTSH (Los Angeles Biomedical Research Institute). On day 26, medium was switched to thyroid maturation medium (Ham's F12 supplemented with 15 mM HEPES, 0.8 mM CaCl₂, 100 ng/ml heparin sodium salt, 0.25% BSA, 50 ng/ml mIGF-1, 5 μ g/ml insulin, 5 μ g/ml ITS, 25 ng/ml hEGF, 50 nM dexamethasone, and 100 mU/ml bTSH) until the harvest day indicated.

Human iPSC Derivation

Procurement of all human specimens was approved by the Institutional Review Boards of the University of Colorado and Boston University. Three

hypothyroid individuals diagnosed with brain-lung-thyroid syndrome arising from mutations in NKX2-1 were identified, and their dermal fibroblasts were reprogrammed with the STEMCCA reprogramming system to generate iPSC lines T1, T3, and T4 (Somers et al., 2010). Control human PSC lines included BU3 (peripheral blood-derived normal iPSC line; from the Center for Regenerative Medicine [CRoM] of Boston University and Boston Medical Center), iPSC17 (fibroblast-derived iPSC) (Crane et al., 2015; gift of Dr. Brian Davis, University of Texas Health Sciences), and RUES2 human ESCs (gift of Dr. Ali Brivanlou, Rockefeller University). Differentiation of human ESC/iPSC into thyroid cells is detailed in the [Supplemental Information](#).

Statistical Analysis

Data are presented as sample means and SDs or SEMs, as indicated in the text and in each figure legend. Sample numbers are also indicated in each case. Differences between groups were analyzed by unpaired two-tailed Student's *t* tests, one-way ANOVA, or two-way ANOVA with Tukey's multiple-comparison post hoc test, as stated in the text or figure legends; *p* < 0.05 was used to indicate significant differences between groups.

SUPPLEMENTAL INFORMATION

Supplemental Information includes Supplemental Experimental Procedures, seven figures, and two tables and can be found with this article online at <http://dx.doi.org/10.1016/j.stem.2015.09.004>.

AUTHOR CONTRIBUTIONS

A.A.K., M.S., A.N.H., and D.N.K. conceived the work, designed experiments, and wrote the manuscript. S.A.R. and A.M.Z. performed *Xenopus* experiments and wrote the manuscript. J.M.S. and S.L. performed mouse foregut explant experiments and wrote the manuscript. M.B. and J.R. designed the Nkx2-1^{mCherry} mouse model. S.U. performed the Tc^{99m} SPECT/CT and MRI experiments. J.C.J., R.R.D., and F.H. procured human cells and developed the human ESC/iPSC model. M.M., F.H., I.A., and L.I. provided critical intellectual input. All authors reviewed, edited, and approved the manuscript.

ACKNOWLEDGMENTS

We dedicate this work to the memory of our co-first author, Dr. Anita Kurmann, who died in a tragic bicycle accident when this manuscript was in the final stages of formatting. Dr. Kurmann was an accomplished endocrine and general surgeon from Switzerland who sought basic science post-doctoral research fellowship training in Boston in the co-mentored setting of the Hollenberg and Kotton laboratories. She was intelligent, well read, kind, humble, and tirelessly committed to her patients, her thyroid research, her family, and her colleagues, who miss her dearly.

We wish to thank the members of the Kotton and Hollenberg labs for insightful discussions. We thank Ron Gluck and Elizabeth Brody-Gluck for project ignition and Dr. Meinrad Busslinger for kindly sharing the Pax8^{Cre} mouse. We thank Brian R. Tilton and Patrick Autissier of the Boston University Flow Cytometry Core Facility for technical assistance and Amulya Iyer of the Kotton lab and Marianne James of the iPS core at the CRoM for maintenance and characterization of patient-specific iPSCs. A.A.K. was supported by a grant from the Swiss National Science Foundation (PBBS P3-146612), L.I. by grant R01 HL111574 and an award co-sponsored by the chILD Foundation/American Thoracic Society, M.B. by a postdoctoral fellowship from the Canadian Institutes of Health Research/Canadian Lung Association/GlaxoSmithKline partnership and from Fonds de Recherche du Québec, A.M.Z. by grant R01 HL114898, and D.N.K. by grants R01 HL095993, R01 HL108678, R01 HL122442, and U01HL110-967.

Received: June 29, 2015

Revised: August 26, 2015

Accepted: September 11, 2015

Published: October 22, 2015

REFERENCES

- Antonica, F., Kasprzyk, D.F., Opitz, R., Iacovino, M., Liao, X.H., Dumitrescu, A.M., Refetoff, S., Peremans, K., Manto, M., Kyba, M., and Costagliola, S. (2012). Generation of functional thyroid from embryonic stem cells. *Nature* 491, 66–71.
- Arufe, M.C., Lu, M., Kubo, A., Keller, G., Davies, T.F., and Lin, R.Y. (2006). Directed differentiation of mouse embryonic stem cells into thyroid follicular cells. *Endocrinology* 147, 3007–3015.
- Arufe, M.C., Lu, M., and Lin, R.Y. (2009). Differentiation of murine embryonic stem cells to thyrocytes requires insulin and insulin-like growth factor-1. *Biochem. Biophys. Res. Commun.* 381, 264–270.
- Bachiller, D., Klingensmith, J., Shneyder, N., Tran, U., Anderson, R., Rossant, J., and De Robertis, E.M. (2003). The role of chordin/Bmp signals in mammalian pharyngeal development and DiGeorge syndrome. *Development* 130, 3567–3578.
- Bilodeau, M., Shojaie, S., Ackerley, C., Post, M., and Rossant, J. (2014). Identification of a proximal progenitor population from murine fetal lungs with clonogenic and multilineage differentiation potential. *Stem Cell Rep.* 3, 634–649.
- Bouchard, M., Souabni, A., and Busslinger, M. (2004). Tissue-specific expression of cre recombinase from the Pax8 locus. *Genesis* 38, 105–109.
- Celli, G., LaRochelle, W.J., Mackem, S., Sharp, R., and Merlino, G. (1998). Soluble dominant-negative receptor uncovers essential roles for fibroblast growth factors in multi-organ induction and patterning. *EMBO J.* 17, 1642–1655.
- Crane, A.M., Kramer, P., Bui, J.H., Chung, W.J., Li, X.S., Gonzalez-Garay, M.L., Hawkins, F., Liao, W., Mora, D., Choi, S., et al. (2015). Targeted correction and restored function of the CFTR gene in cystic fibrosis induced pluripotent stem cells. *Stem Cell Rep.* 4, 569–577.
- Fagman, H., and Nilsson, M. (2010). Morphogenesis of the thyroid gland. *Mol. Cell. Endocrinol.* 323, 35–54.
- Fagman, H., Liao, J., Westerlund, J., Andersson, L., Morrow, B.E., and Nilsson, M. (2007). The 22q11 deletion syndrome candidate gene Tbx1 determines thyroid size and positioning. *Hum. Mol. Genet.* 16, 276–285.
- Goss, A.M., Tian, Y., Tsukiyama, T., Cohen, E.D., Zhou, D., Lu, M.M., Yamaguchi, T.P., and Morrisey, E.E. (2009). Wnt2/2b and beta-catenin signaling are necessary and sufficient to specify lung progenitors in the foregut. *Dev. Cell* 17, 290–298.
- Green, M.D., Chen, A., Nostro, M.C., d'Souza, S.L., Schaniel, C., Lemischka, I.R., Gouon-Evans, V., Keller, G., and Snoeck, H.W. (2011). Generation of anterior foregut endoderm from human embryonic and induced pluripotent stem cells. *Nat. Biotechnol.* 29, 267–272.
- Hamvas, A., Deterding, R.R., Wert, S.E., White, F.V., Dishop, M.K., Alfano, D.N., Halbower, A.C., Planer, B., Stephan, M.J., Uchida, D.A., et al. (2013). Heterogeneous pulmonary phenotypes associated with mutations in the thyroid transcription factor gene NKX2-1. *Chest* 144, 794–804.
- Hilfer, S.R., Iszard, L.B., and Hilfer, E.K. (1968). Follicle formation in the embryonic chick thyroid. II. Reorganization after dissociation. *Z. Zellforsch. Mikrosk. Anat.* 92, 256–269.
- Huang, S.X., Islam, M.N., O'Neill, J., Hu, Z., Yang, Y.G., Chen, Y.W., Mumau, M., Green, M.D., Vunjak-Novakovic, G., Bhattacharya, J., and Snoeck, H.W. (2014). Efficient generation of lung and airway epithelial cells from human pluripotent stem cells. *Nat. Biotechnol.* 32, 84–91.
- Jiang, N., Hu, Y., Liu, X., Wu, Y., Zhang, H., Chen, G., Liang, J., Lu, X., and Liu, S. (2010). Differentiation of E14 mouse embryonic stem cells into thyrocytes in vitro. *Thyroid* 20, 77–84.
- Kameda, Y., Ito, M., Nishimaki, T., and Gotoh, N. (2009). FRS2alpha is required for the separation, migration, and survival of pharyngeal-endoderm derived organs including thyroid, ultimobranchial body, parathyroid, and thymus. *Dev. Dyn.* 238, 503–513.
- Krude, H., Schütz, B., Biebermann, H., von Moers, A., Schnabel, D., Neitzel, H., Tönnies, H., Weise, D., Lafferty, A., Schwarz, S., et al. (2002). Choreoathetosis, hypothyroidism, and pulmonary alterations due to human NKX2-1 haploinsufficiency. *J. Clin. Invest.* 109, 475–480.
- Lancaster, M.A., and Knoblich, J.A. (2014). Organogenesis in a dish: modeling development and disease using organoid technologies. *Science* 345, 1247125.
- Lania, G., Zhang, Z., Huynh, T., Caprio, C., Moon, A.M., Vitelli, F., and Baldini, A. (2009). Early thyroid development requires a Tbx1-Fgf8 pathway. *Dev. Biol.* 328, 109–117.
- Longmire, T.A., Ikonomou, L., Hawkins, F., Christodoulou, C., Cao, Y., Jean, J.C., Kwok, L.W., Mou, H., Rajagopal, J., Shen, S.S., et al. (2012). Efficient derivation of purified lung and thyroid progenitors from embryonic stem cells. *Cell Stem Cell* 10, 398–411.
- Ma, R., Latif, R., and Davies, T.F. (2009). Thyrotropin-independent induction of thyroid endoderm from embryonic stem cells by activin A. *Endocrinology* 150, 1970–1975.
- Ma, R., Latif, R., and Davies, T.F. (2013). Thyroid follicle formation and thyroglobulin expression in multipotent endodermal stem cells. *Thyroid* 23, 385–391.
- Ma, R., Latif, R., and Davies, T.F. (2015). Human embryonic stem cells form functional thyroid follicles. *Thyroid* 25, 455–461.
- Mallette, J.M., and Anthony, A. (1966). Growth in culture of trypsin dissociated thyroid cells from adult rats. *Exp. Cell Res.* 41, 642–651.
- Martin, A., Valentine, M., Unger, P., Lichtenstein, C., Schwartz, A.E., Friedman, E.W., Shultz, L.D., and Davies, T.F. (1993). Preservation of functioning human thyroid organoids in the scid mouse: 1. System characterization. *J. Clin. Endocrinol. Metab.* 77, 305–310.
- McCracken, K.W., Catá, E.M., Crawford, C.M., Sinagoga, K.L., Schumacher, M., Rockich, B.E., Tsai, Y.H., Mayhew, C.N., Spence, J.R., Zavros, Y., and Wells, J.M. (2014). Modelling human development and disease in pluripotent stem-cell-derived gastric organoids. *Nature* 516, 400–404.
- Murry, C.E., and Keller, G. (2008). Differentiation of embryonic stem cells to clinically relevant populations: lessons from embryonic development. *Cell* 132, 661–680.
- Pagliuca, F.W., Millman, J.R., Gürtler, M., Segel, M., Van Dervort, A., Ryu, J.H., Peterson, Q.P., Greiner, D., and Melton, D.A. (2014). Generation of functional human pancreatic β cells in vitro. *Cell* 159, 428–439.
- Parlato, R., Rosica, A., Rodriguez-Mallon, A., Affuso, A., Postiglione, M.P., Arra, C., Mansouri, A., Kimura, S., Di Lauro, R., and De Felice, M. (2004). An integrated regulatory network controlling survival and migration in thyroid organogenesis. *Dev. Biol.* 276, 464–475.
- Petryk, A., Anderson, R.M., Jarcho, M.P., Leaf, I., Carlson, C.S., Klingensmith, J., Shawlot, W., and O'Connor, M.B. (2004). The mammalian twisted gastrulation gene functions in foregut and craniofacial development. *Dev. Biol.* 267, 374–386.
- Postiglione, M.P., Parlato, R., Rodriguez-Mallon, A., Rosica, A., Mithbaokar, P., Maresca, M., Marians, R.C., Davies, T.F., Zannini, M.S., De Felice, M., and Di Lauro, R. (2002). Role of the thyroid-stimulating hormone receptor signaling in development and differentiation of the thyroid gland. *Proc. Natl. Acad. Sci. U S A* 99, 15462–15467.
- Serls, A.E., Doherty, S., Parvatiyar, P., Wells, J.M., and Deutsch, G.H. (2005). Different thresholds of fibroblast growth factors pattern the ventral foregut into liver and lung. *Development* 132, 35–47.
- Shifley, E.T., Kenny, A.P., Rankin, S.A., and Zorn, A.M. (2012). Prolonged FGF signaling is necessary for lung and liver induction in *Xenopus*. *BMC Dev. Biol.* 12, 27.
- Somers, A., Jean, J.C., Sommer, C.A., Omari, A., Ford, C.C., Mills, J.A., Ying, L., Sommer, A.G., Jean, J.M., Smith, B.W., et al. (2010). Generation of Transgene-Free Lung Disease-Specific Human iPS Cells Using a Single Excisable Lentiviral Stem Cell Cassette. *Stem Cells* 28, 1728–1740.

Trueba, S.S., Augé, J., Mattei, G., Etchevers, H., Martinovic, J., Czernichow, P., Vekemans, M., Polak, M., and Attié-Bitach, T. (2005). PAX8, TITF1, and FOXE1 gene expression patterns during human development: new insights into human thyroid development and thyroid dysgenesis-associated malformations. *J. Clin. Endocrinol. Metab.* *90*, 455–462.

Vitelli, F., Taddei, I., Morishima, M., Meyers, E.N., Lindsay, E.A., and Baldini, A. (2002). A genetic link between Tbx1 and fibroblast growth factor signaling. *Development* *129*, 4605–4611.

Wendl, T., Adzic, D., Schoenebeck, J.J., Scholpp, S., Brand, M., Yelon, D., and Rohr, K.B. (2007). Early developmental specification of the thyroid gland depends on hox-expressing surrounding tissue and on FGF signals. *Development* *134*, 2871–2879.

Zuckier, L.S., Dohan, O., Li, Y., Chang, C.J., Carrasco, N., and Dadachova, E. (2004). Kinetics of perrhenate uptake and comparative biodistribution of perrhenate, pertechnetate, and iodide by Nal symporter-expressing tissues in vivo. *J. Nucl. Med.* *45*, 500–507.